Published in final edited form as:
OMICS. 2010 February ; 14(1): 75–90. doi:10.1089/omi.2009.0115.

Ginkgo Biloba Extract Induces Gene Expression Changes in Xenobiotics Metabolism and the Myc-centered Network

Lei Guo[a,*], **Nan Mei**[b], **Wayne Liao**[c], **Po-Chuen Chan**[d], and **Peter P. Fu**[e,*]

[a]Division of Systems Toxicology, National Center for Toxicological Research, FDA, Jefferson, AR 72079, USA

[b]Division of Genetic and Reproductive Toxicology, National Center for Toxicological Research, FDA, Jefferson, AR 72079, USA

[c]PhalanxBio, Inc., 1400 Page Mill Road, Palo Alto, CA 94304, USA

[d]National Institute of Environmental Health Sciences, Research Triangle Park, NC 27709, USA

[e]Division of Biochemical Toxicology, National Center for Toxicological Research, FDA, Jefferson, AR 72079, USA

Abstract

The use of herbal dietary supplements in the United States is rapidly growing and it is crucial that the quality and safety of these preparations be ensured. To date, it is still a challenge to determine the mechanisms of toxicity induced by mixtures containing many chemical components, such as herbal dietary supplements. We previously proposed that analyses of the gene expression profiles using microarrays in the livers of rodents treated with herbal dietary supplements is a potentially practical approach for understanding the mechanism of toxicity. In this study, we utilized microarrays to analyze gene expression changes in the livers of male B6C3F1 mice administered *Ginkgo biloba* leaf extract (GBE) by gavage for two years, and to determine pathways and mechanisms associated with GBE treatments. Analysis of 31,802 genes revealed that there were 129, 289, and 2011 genes significantly changed in the 300, 600, and 2,000 mg/kg treatment groups, respectively, when compared with control animals. Drug metabolizing genes were significantly altered in response to GBE treatments. Pathway and network analyses were applied to investigate the gene relationships, functional clustering, mechanisms involved in GBE exposure. These analyses indicate alteration in the expression of genes coding for drug metabolizing enzymes, the NRF2- mediated oxidative stress response pathway, and the Myc gene-centered network named “cell cycle, cellular movement and cancer” were found. These results indicate that *Ginkgo biloba* related drug metabolizing enzymes may cause herb-drug interactions and contribute to hepatotoxicity. In addition, the outcomes of pathway and network analysis may be used to elucidate the toxic mechanisms of *Ginkgo biloba*.

Keywords

Ginkgo biloba extract; microarray; gene expression; drug metabolizing gene; pathway analysis; network analysis

[*]Corresponding authors. Tel: +1 870 543 7048, lei.guo@fda.hhs.gov (L. Guo); Tel: +1 870 543 7027, peter.fu@fda.hhs.gov (P. Fu).

Conflict of interest statement The authors declare that there is no conflict of interest.

Introduction

Since the U.S. Congress passed the Dietary Supplement Health and Education Act (DSHEA) in 1994, herbal products have been the fastest growing segment of the vitamin, mineral supplements, and herbal products industry in the United States. In 2004, the American Herbal Products Association estimated that there were about 3,000 species of plants in as many as 50,000 different products sold as herbal supplements in the United States (Zurer and Hanson, 2004). St John's wort, *Ginkgo biloba*, golden seal, *panax* ginseng, kava, Aloe vera, and mild thistle extract are among the most widely used of these products (Chan and Fu, 2007; Chan et al., 2007; Fu et al., 2008; Guo et al., 2009).

Although it has been reported that a number of herbal dietary supplements cause adverse health effects (Chan and Fu, 2007; Chan et al., 2007; Fu, 2007; Fu et al., 2007; Fu et al., 2008; Gurley et al., 2005; Gurley et al., 2007; Hu et al., 2005; Singh, 2005), to date, safety issues concerning potential side-effects and toxic contamination of herbal products have not been adequately addressed. Thus, assessment of the safety of herbal plants and herbal dietary supplements is timely and important (FDA, 2001; FDA, 2004a; FDA, 2004b; Fong, 2002; Fu et al., 2002). Recently, a number of herbal dietary supplements and active ingredients have been nominated by the U.S. Food and Drug Administration (FDA) and the U.S. National Institutes of Health (NIH) to the National Toxicology Program (NTP) for determination of their toxicity and tumorigenicity. *Ginkgo biloba*, *panax* ginseng, kava, Aloe vera, and green tea are among the herbal dietary supplements currently under investigation by the NTP.

In general, approaches for determining the mechanism by which a pure chemical induces toxicities or tumors have been well established. Nevertheless, it is still a challenge to determine the mechanisms of toxicities or tumor induction elicited by a mixture of many chemical components, such as herbal plants and herbal dietary supplements. For chemical mixtures there is a need for new approaches for elucidating mechanisms. Toward this goal, we previously examined the alterations in gene expression of drug metabolizing enzymes in the livers of Fischer 344 rats administered kava extract by gavage for 14 weeks (Guo et al., 2009). Our results indicate that kava extract can significantly modulate drug metabolizing enzymes, which can potentially cause herb-drug interactions and may be responsible for different types of liver injuries. The gene expression profile correlated well (Guo et al., 2009) with immunohistochemical data collected using the same liver tissues (Clayton et al., 2007). We observed that kava altered the expression of Cyp1a1 (Cytochrome p450 1a1) and many other Cyp enzymes that metabolize various xenobiotics and drugs, and the changes for many of those genes were first reported by us (Guo et al., 2009). These findings illustrate that, without obtaining the whole spectrum of gene expression changes, some important information may be missed. Our study also suggested that analysis of the gene expression profiles using microarrays in the livers of rodents treated with herbal dietary supplements is a potentially practical approach for understanding the mechanism of toxicity (Guo et al., 2009).

Ginkgo biloba has been one of the most widely sold products in health food stores in the United States, with total sales exceeding $100 million (Chan et al., 2007). Several reports have indicated that *Ginkgo biloba* inhibits Cyp activity and, when taken in combination with prescription and conventional medications, may produce Cyp-mediated herb-drug interactions (Bressler, 2005; Gurley et al., 2005; Gurley et al., 2007; Hu et al., 2005; Matthias et al., 2007; Singh, 2005; Williamson, 2005; Wold et al., 2005; Zou et al., 2002). *Gingko biloba* leaf extract was nominated by the National Cancer Institute to the NTP to conduct toxicological evaluation, mechanistic studies, and a two-year chronic carcinogenicity bioassay based on the following reasons: (1) *Ginkgo biloba* is a well-defined

product and itself or its active ingredients have clearly demonstrated biological activities; (2) *Ginkgo biloba* can be consumed in rather large doses for an extended period of time; and (3) some ingredients in *Ginkgo biloba* are known mutagens (NTP, 1998). As a continuation of our mechanistic studies of herbal dietary supplements, in the present study, gene expression changes were analyzed with the focus on drug metabolizing genes in the livers of male B6C3F1 mice treated orally and chronically with *Ginkgo biloba* extract. In addition, changes in pathways and networks, which may indicate toxicity, were also explored.

Materials and methods

Ginkgo biloba leaf extract preparation and animal treatment

Ginkgo biloba leaf extract (GBE) (CAS No. 90045-36-6) was received from the Midwest Research Institute (MRI, Kansas City, MO). Infrared spectroscopy and HPLC/UV analyses confirmed the chemical was GBE by comparing with a reference sample received from MRI. The identity, chemical purity, and formulation analysis evaluation data are available at the archives of the National Institute of Environmental Health Sciences. Male B6C3F1 mice (38-44 days old) were obtained from Taconic Laboratory Animals and Services (Germantown, NY) and were used in the NTP toxicity and carcinogenesis studies of GBE in mice. The animals were quarantined for 14 days before separating at random into 4 groups. GBE in corn oil was administered to each group by gavage at 0, 200, 600, or 2,000 mg/kg, 5 days a week for 104 weeks. The animals were monitored twice daily during the course of the experiment, and body weights and clinical observations were recorded weekly for the first 13 weeks and every four weeks thereafter, and at the study termination. Animal handling and husbandry were conducted in accordance with guidelines of the National Institutes of Health. During necropsy at terminal sacrifice (104 weeks) a piece of the left lateral lobe of the liver was collected from 10 animals from each group, cut into 3 pieces and frozen in liquid nitrogen until use.

RNA isolation and quality control

Total RNA was isolated from liver tissues of control and GBE-treated mice using an RNeasy kit (Qiagen, Valencia, CA). The RNA was quantified by optical density reading using a NanoDrop ND-1000 spectrophotometer (NanoDrop products, Wilmington, DE). The purity and quality of extracted RNA were evaluated using the RNA 6000 LabChip and Agilent 2100 Bioanalyzer (Agilent Technologies, Palo Alto, CA). RNA samples with RNA integrity numbers (RINs) greater than 9.0 were used for target labeling, microarray experiments, and TaqMan assays.

Preparation of cyanine 5 (Cy5)-labeled aRNA for array hybridization

Five μg of RNA from each sample was used for Cy5-labeled aRNA preparation using the Ambion MessageAmp aRNA Amplification Kit (Applied Biosystems Inc, Foster City, CA)) with minor modifications to adopt the amino-allyl UTP indirect labeling protocol. In brief, the 4 μl T7 UTP solution (75 mM) was replaced with 2 μl of T7 UTP solution (75 mM) and 3 μl of 50 mM 5-(3-aminoallyl)-UTP in the process of *in vitro* transcription to synthesize aRNA. The reaction conditions and the purification of un-labeled aRNA remained the same as described in the user's manual. For Cy5 labeling of aRNA, 40 μg of un-labeled aRNA was used in each labeling reaction to generate sufficient Cy5-labeled cRNA for the microarray hybridization in triplicate. The Cy5 dye (GE Healthcare, Piscataway, NJ) was suspended in 32 μl DMSO before use. Eight μl of Cy5 dye solution and 2.5 μl of 10 μM NaOH were added to the 40 μg aRNA and the volume was adjusted to 25 μl by addition of ddH_2O. The mixture was incubated at 25°C in the dark for 2 hours. The labeled cRNA was then purified using the Ambion NucAway Spin Column (ABI). The amount and labeling efficiency of the purified Cy5-labeled cRNA were quantified by optical density reading

using a NanoDrop ND-1000. The minimal requirement of labeling efficiency was 10 Cy5 dye molecules per 1,000 nucleotides.

Hybridization of labeled cRNA to microarrays and microarray imaging

Microarray experiments were performed using Phalanx Mouse OneArray Version 1.1 (MOA 1.1; Phalanx Biotech Group, Inc., HsinChu, Taiwan). Each microarray contains 31,802 oligonucleotide probes that include 29,922 mouse gene probes for transcription expression profiling and 1880 experimental control probes. The MOA 1.1 content is based on an abridged version of the Mouse Exonic Evidence Based Oligonucleotide (MEEBO). MEEBO consists of a set of 70-mer probes made available to the public specifically for DNA microarray. For microarray hybridization experiments, 10 μg Cy5-labeled cRNA derived from each RNA sample was applied to each of three MOA 1.1 microarrays. Prior to the microarray hybridization, the Cy5-labeled cRNAs were fragmented using the reagents and protocol provided in Ambion RNA Fragmentation Reagents kit (Ambion Inc.). Each 10 μg fragmented Cy5-labeled cRNA were suspended in OneArray hybridization buffer at a final volume of 180 μl for microarray hybridization. After microarray hybridization, the arrays were scanned using a fluorescence scanner (GenePix 4000B; Molecular Devices, Sunnyvale, CA) and the fluorescent intensities were extracted from the generated images by following the instructions and the conditions described in the MOA 1.1 User's Manual.

Microarray data analysis

Each Cy5-labeled cRNA derived from a liver RNA sample was hybridized to MOA 1.1 microarrays in triplicate. The raw microarray intensity data was imported to into ArrayTrack (http://www.fda.gov/nctr/science/centers/toxicoinformatics/ArrayTrack/). The intensities of the three technical replicates for each probe were averaged and then normalized by quantile normalization. Differentially expressed genes (DEGs) were selected based on *t*-test and fold-change cutoff criteria. Principal Component Analysis (PCA) and Hierarchical Cluster Analysis (HCA) were conducted within ArrayTrack. Additional calculations were performed within JMP 7.0 (SAS Institute, Cary, NC). The pathways, networks and functional analyses were generated through the use of Ingenuity Pathways Analysis (IPA, Ingenuity Systems, www.ingenuity.com). Canonical pathways analysis identified the pathways from the IPA library of canonical pathways that were most significant to the data set. DEGs that associated with a canonical pathway in the IPA Base were considered for the analysis. The significance of the association between the data set and the canonical pathway was measured in two ways: 1) a ratio of the number of genes from the data set that map to the pathway divided by the total number of genes that map to the canonical pathway is displayed, and 2) Fischer's exact test was used to calculate a *p*-value determining the probability that the association between the genes in the dataset and the canonical pathway is explained by chance alone. DEGs containing gene identifiers and corresponding expression values were uploaded into the application to generate networks. Each gene identifier was mapped to its corresponding gene object in the Ingenuity Pathways Knowledge Base. These genes, called focus genes, were overlaid onto a global molecular network developed from information contained in the Ingenuity Pathways Knowledge Base. Networks of these focus genes were then algorithmically generated based on their connectivity.

TaqMan gene expression assays

DEGs identified with microarray analysis were selectively confirmed by TaqMan assays (Applied Biosystems, Foster City, CA). Eleven TaqMan probes were used in these assays, including Cyp1a1 (Mm00487218_m1), Cyp1a2 (Mm00487224_m1), Cyp2b10 (Mm00456591_m1), Cp2b13 (Mm00771172_g1), Cyp2c55 (Mm00472168_m1), Cyp2d13 (Mm00775259_gl), Ces2 (Mm00524035_m1), Fmo3 (Mm00514964_m1), Gsta2

(Mm00833353_mH), Actb (Mm00607939_s1), and Polr2a (Mm 00839493_m1). Actb and Polr2a were used as endogenous controls. cDNA was prepared using a High-Capacity cDNA Archive Kit (Applied Biosystems), i.e., 2 μg RNA was reverse-transcribed in a final volume of 20 μl with random primers at 25°C for 10 min followed by 37°C for 120 min according to the manufacturer's instructions. Each TaqMan assay was run in triplicate for each RNA sample. Total cDNA (25 ng) in a 25 μl final volume was used for each assay. Assays were run with Universal Master Mix (2X) without AmpErase UNG on an Applied Biosystems 7900 HT Real-Time PCR System using universal cycling conditions (10 min at 95°C; 15 sec at 95°C, 1 min 60°C, 40 cycles).

TaqMan data normalization and analysis

Two endogenous control genes, β-actin (Actb) and RNA polymerase II A (Polr2a), were used for normalization. Each replicate cycle threshold (C_T) was normalized to the average C_T of the two endogenous controls on a per sample basis. The comparative C_T method (Livak and Schmittgen, 2001) was used to calculate relative quantification of gene expression. The following formula was used to calculate the relative amount of the transcripts in the GBE-treated sample (treated) and the vehicle-treated sample (control), and both were normalized to the endogenous controls: $\Delta\Delta C_T = \Delta C_T$ (treated) - ΔC_T (control), where ΔC_T is the difference in C_T between the target gene and endogenous controls by subtracting the average C_T of controls. The fold-change for each treated sample relative to the control sample = $2^{-\Delta\Delta C_T}$. A list of DEGs was identified using a two-tailed *t*-test. The criteria were *P* value less than 0.05 and a mean difference equal to or greater than 2-fold.

Results

Animals

During the course of the study no clinical findings attributed to GBE administration were observed. After 18-19 months of GBE treatment, the body weights of the 600 and 2,000 mg/kg mice began to decrease gradually. At terminal sacrifice the body weights of these 2 dose groups of mice were significantly lower (~17% and ~25%, respectively) compared with controls.

Microarray data quality assessment

In this study, the global changes of gene expression in mouse liver treated with GBE were determined by high-density oligonucleotide microarray analysis (Mouse OneArray which contains 31,802 probes covering 29,922 verified mouse genes). Total RNA was isolated from liver tissues of control mice and mice treated with 200, 600, and 2,000 mg/kg GBE. Each group consisted of four animals; therefore, 16 RNA samples were isolated for microarray analysis. Three technical replicate arrays were performed for each RNA sample and thus a total of 48 microarrays were used in this study.

The overall quality of data from the 48 microarrays was first assessed by Hierarchical Cluster Analysis (HCA). The $\log_2$ intensity of the entire gene set including 31,802 probes was scaled by *Z*-score transformation, and then these values were hierarchically clustered using a distance metric of 1-R, where R is the Pearson correlation coefficient between two samples, and the average linkage (Figure 1). As expected, for most samples, the 3 technical replicates for the same RNA sample were tightly grouped, indicating close similarity among them. In addition, two apparent clusters were revealed. The first cluster (in black and red) consists of samples from the control, and low- (200 mg/kg) and middle-dose (600 mg/kg) GBE treatments; the second cluster (in blue) includes samples from high-dose (2,000 mg/kg) GBE treatments. Samples in the high dose group were clearly separated from those in the

control, low and middle groups (Figure 1). In the first big cluster, the three subgroups (control, low- and middle-dose) were also well separated with few exceptions.

The reproducibility of the three technical replicates was further assessed by calculating the Pearson correlation coefficient of pair-wise $\log_2$ intensity. R values of each pair-wise comparison were obtained; the median R values of the three technical replicates are shown in Table 1. The median R values across 16 RNA samples range from 0.984-0.997. One array from sample C38 (C38_3) and one from C24 (C24_2) showed dissimilarity in comparison with its other two technical replicates with relatively low correlation coefficients (0.979 and 0.965, respectively). These two hybridizations were considered as outliers and were removed from further calculation and data analysis.

It is worth noting that the intensities of all data points (31,802 probes) were included for the comparison. No specific cutoff was applied for evaluation of microarray quality. For visualization purpose, as an example, the raw $\log_2$ intensity data of all 31,802 probes from the three technical replicates (C20_0_1, C20_0_2, and C20_0_3) of animal #C20 were plotted against each other (Figure 2). As shown in the scatter plot, for most spots, the intensity values from the replicate microarrays accumulated along the diagonal axis with a correlation >0.996, indicating that the data from the technical microarrays were highly reproducible.

Profiling of gene expression

The intensity values of each probe from the three technical replicates were averaged and $\log_2$ transformed. The overall quality of the microarray data from the 16 RNA samples was further assessed by calculating the Pearson correlation coefficients of the averaged $\log_2$ intensity data for all pair-wise sample comparisons within each control or treatment group (Table 2). The median correlation coefficient was 0.973 across all 16 arrays with a range from 0.926 to 0.989. The median correlation for the control group was 0.987 with a range from 0.983 to 0.988, whereas the median correlation for the 2,000 mg/kg treatment group was 0.970 with a range from 0.961 to 0.977. These results demonstrated the high degree of gene expression similarity for samples within the same group. On the other hand, the median correlation between the control group and the 2,000 mg/kg GBE treated group was 0.957 with a range from 0.933 to 0.964, demonstrating that there were significant differences in the gene expression profiles between the control and high dose GBE treated groups.

The $\log_2$ transformed intensity of any two gene expression profiles was plotted and compared as shown in Figure 3. When intensities of the entire probe set obtained from a control sample (C20) were plotted against another control sample (C36), most of data points gathered along the diagonal axis of the scatter plot with a correlation coefficient value of 0.987, demonstrating the good repeatability of the two biological replicates (Figure 3A). However, in comparison between the control sample (C20) and the 2,000 mg/kg GBE treated sample (C32), many data points were scattered, indicating a great number of genes were altered in response to the treatment of high dose GBE (Figure 3B).

The intensities of the gene expression data were also analyzed by Principal Component Analysis (PCA). PCA uses analysis of the principal sources of variance in data and displays this information graphically either in a 2-dimensional or 3-dimensional space, which is most commonly used to classify gene expression profiles (Wang and Gehan, 2005). Figure 4 displays a PCA 3D view using the first three principal components for gene expression profiles from the samples. The PCA result showed a clear separation between controls and 2,000 mg/kg treated samples, suggesting that there was a treatment effect on liver gene expression which is consistent with the results from the HCA (Figure 1). Less separation

was observed between controls, low dose (i.e. 200 mg/kg), and middle dose (i.e. 600 mg/kg) groups based on PCA.

Differentially expressed genes (DEGs)

The average intensities for each probe from three technical replicates of each sample were normalized by the quantile normalization method, which assumes that a quantile plot of two data vectors with the same distribution will have a straight diagonal line. The normalized data were used for selection of DEGs. We had reported that a straightforward approach of fold-change selection plus a nonstringent *P* cutoff is useful in identifying reproducible gene lists (Guo et al., 2006; Shi et al., 2006). We used a 2-fold change in gene expression compared to the controls and a *P*-value less than 0.01 for the difference as minimum requirements for the selection of DEGs. Based on these two criteria a total of 129, 289, and 2,011 genes, respectively, in 200, 600, and 2,000 mg/kg treatment groups satisfied the requirements and were identified as DEGs. Out of 2,011 genes identified in the 2,000 mg/kg treatment group, 817 were up-regulated and 1194 genes were down-regulated in response to GBE exposure. Significance Analysis of Microarray (SAM) (Tusher et al., 2001), the statistical method which calculates difference in gene expression based on permutation analysis of expression data and calculates a false discovery rate, was also applied to generate DEGs. With a FDR of 0.01 and fold-change greater than 2, a total of 2211 genes were identified in 2000 mg/kg treatment group comparing to control group. Out of 2011 genes were indentified as DEGs using the *t*-test, 1952 genes (97%) are overlapped with those produced by the SAM, indicating the similar gene lists were produced with two gene selection methods.

Since metabolic activation of chemicals is very important for liver toxicity and alteration of drug metabolizing genes is suspected to contribute to the toxicity of *Gingko biloba*, we first focused our investigation on the gene expression changes of drug metabolizing enzymes and found that the expression of a large number of drug metabolizing genes was altered. Table 3 lists the 68 drug metabolizing genes whose expression was significantly altered by 2,000 mg/kg GBE treatment. Among the 68 altered genes, 36 genes were up-regulated and 32 genes were down-regulated. As tabulated in Table 3, among the 68 drug metabolizing enzyme associated genes, 33 genes are Phase I metabolizing enzymes; 18 genes are Phase II metabolizing enzymes; and 17 genes are transporters (Phase III). As summarized in Table 4, 21% (33 out of 154) of Phase I genes, 21% (18 out of 87) of Phase II genes, and 24% (17 out of 72) of Phase III genes were altered. Although a relatively small portion of genes (6.7%) were altered at the genome level (2011 DEGs out of 29,922 probes), the percentage of changed drug metabolizing genes (22%, Table 4) was high.

Real-time PCR validation

TaqMan assays were used to verify the results for a selected group of genes whose expression changes were seen using microarrays. Nine drug metabolizing genes were selected for the TaqMan validation. The results are shown in Figure 5A. Based on triplicate measurements for each RNA sample, the genes Cyp1a1, Cyp1a2, Cyp2b10, Cyp2c55, Ces2, and Gsta2 were over-expressed, and the changes in Cyp1a1, Ces2, and Gsta2 were dose dependent. The expression of Cyp2b13, Cyp2d13, and Fmo3 genes were decreased, notably for the highest dose treatment (Figure 5B). Over 100-fold decrease in gene expression was observed for the three down-regulated genes in the 2,000 mg/kg treatment group. As expected, TaqMan data were in good agreement with the microarray data (Figure 5 and Table 3).

Pathway analysis

Ingenuity Pathway Analysis (IPA, version 7.0) was used to determine the most relevant biological functions, pathways, and networks of the genes altered by 2,000 mg/kg GBE treatment. Out of 2011 DEGs, 1246 were identified by IPA and were overlaid onto a global molecular network developed from information contained in the database. Not to our surprise, the top canonical pathway was “metabolism of xenobiotics by cytochrome P450” with 36 genes involved and a *P*-value of 1.26E-11 followed by “fatty acid metabolism” (Table 5 and Supplementary data). Interestingly, NRF2 (nuclear factor erythroid-related factor 2)-mediated oxidative stress response was identified with 23 genes involved and a *P*-value of 5.37E-03. In the pathway regulated by NRF2, most of the genes were up-regulated while two genes were down-regulated (Figure 6). The up-regulated genes included those coding for detoxifying enzymes (Nqo1, Gstms, Gstas, Gstp1, and Ugt1a2), glutathione homeostasis (Gsr) and transporter (Abcb1). Maf2, a transcriptional factor forms heterodimers with Nrf2, was also up-regulated. The two down-regulated genes were P13k, which plays a role in Nrf2 phosphorylation, and Sod3, which is a family member of antioxidants. Nqo1 showed a prominent change in expression, exhibiting 7.5- and 11-fold induction for 600 and 2000 mg/kg treatments, respectively.

The significantly changed genes after GBE administration were mapped into 87 networks. Each network was associated with specific genes and involved different functions. Twenty-three networks had 20 or more focus molecules. The first network, which contains the largest number of genes (34 genes), with functions related to “cell cycle, cellular movement and cancer”, as illustrated in Figure 7. The central gene in this network is Myc, the pro-oncogene, which was up-regulated by about 6-fold. Twenty-one genes were found to be associated directly with Myc and these genes function in cell cycle, cell growth/proliferation, and cell death processes. Out of these 21 Myc-associated genes, 15 were up-regulated and 6 were down-regulated. Notably, Cidec (cell-death-inducing DFFA-like effectors c), which promotes apoptosis, exhibited a 47-fold induction. Known molecules of DNA replication checkpoint (Cdca8 and Cdc45l) were also up-regulated. Gene Gas1 (growth arrest-specific 1), the tumor suppressor gene that blocks entry to S phase and prevents cycling of cells, was remarkably down-regulated by 20-fold.

Discussion

Currently there is no established methodology for determining the mechanisms of toxicity (particularly tumorigenicity) induced by a mixture contains many chemical components, such as GBE and other herbal plant extracts. Previously, we have proposed that DNA microarray analysis should be a highly practical initial approach for revealing the whole spectrum of gene expression alterations by a chemical mixture (Guo et al., 2009). Microarray technology is a useful tool to rapidly detect the induction/inhibition of drug metabolizing enzymes after toxicant treatment, and it has greatly contributed to the understanding of drug metabolizing enzyme function and expression (Blomme et al., 2009; Rezen et al., 2007). Although levels of gene expression do not fully represent the levels of enzyme activities, investigations at the gene expression level have revealed that there is a high degree of correlation for Phase I enzymes between the fold inductions of the enzymatic activity and mRNA expression in liver samples (Iyer and Sinz, 1999; Roymans et al., 2004).

In this study, we analyzed gene expression changes in the livers of B6C3F1 mice treated chronically with 200, 600 and 2,000 mg/kg of GBE for 2 years using a genome-wide microarray approach. A total of 31,802 probes covering 29,922 verified mouse genes were analyzed and three technical replicate arrays were performed for each RNA samples. The results of Hierarchical Cluster Analysis (Figure 1), Pearson’s correlation coefficient of pair-wise $\log_2$ intensity correlation (Table 1), and scatter plotting of the overall gene expression

profiles (Figure 2) demonstrated the high quality and reproducibility of DNA microarray data obtained from the three technical replicates.

When the gene expression results GBE-treated rats were compared to the controls, a total of 2011 genes in the 2,000 mg/kg treatment group were differentially expressed, of which there were 68 drug metabolizing enzyme associated genes, with 33, 18, and 17 genes belonging to Phase I, Phase II, and Phase III, respectively (Table 3). It is worth noting that 23 out of the 33 expressed Phase I metabolism associated genes were the Cyps, in which 2 genes belong to the Cyp1 superfamily (Cyp1a1 and 1a2), 15 genes belong to the Cyp2 superfamily, and 2 genes belong to the Cyp3 superfamily (Table 3). The Cyp1, Cyp2, and Cyp3 superfamilies are the most important metabolizing enzymes in the metabolism of drugs and the metabolic activation of toxic and carcinogenic xenobiotics (Gonzalez and Gelboin, 1994;Gonzalez and Yu, 2006).

One of the most reported adverse effects caused by herbal products is hepatotoxicity. While the mechanism of hepatotoxicity initiated by herbal products is not clear, modulation of drug-metabolizing enzymes, leading to herb-drug interactions, is probably one of the major causes (Clayton et al., 2007; Clouatre, 2004; Guo et al., 2009). The alteration of a number of drug metabolizing enzymes by GBE treatment (Table 3) could potentially lead to herb-drug interactions as well as changes in the metabolic activation of carcinogenic chemicals when concomitantly present in the body. Our results are consistent with the report that Ginkgo *biloba* modulated Cyp 450 enzyme activity and consequently may produce Cyp-mediated herb-drug interactions (Dubey et al., 2004; Gurley et al., 2004; Gurley et al., 2005; Zou et al., 2002).

It is well established that the Cyp1 superfamily is important in the metabolism of xenobiotics, and the members of Cyp2 and Cyp3 superfamilies catalyze metabolism of drugs and other substances. Cyp1a1, which generally exists in a very low amount in the adult liver (Martignoni et al., 2006), was dramatically induced by GBE treatment, as detected by both the microarray analysis and TaqMan assay (Table 3 and Figure 3A). Cyp1a1 and Cyp1a2 are regulated by AHR, the aryl hydrocarbon receptor, which plays an important role in cell cycle regulation, apoptosis and development (Xu et al., 2005). It is evident that some toxins such as tumorigenic polycyclic aromatic hydrocarbons (PAHs) (Martignoni et al., 2006) and carcinogen 2,3,7,8-tetrachlorodibenzo-p-dioxin (TCDD) are able to induce Cyp1a1 through AHR, and the upregulation of Cyp1a1 is considered the indicator of TCDD-induced carcinogenesis (Brunnberg et al., 2006). Thus, induction of Cyp1a1 may contribute to the toxic mechanism of *Ginkgo biloba*, and/or may enhance metabolic activation of the hazardous tumorigenic xenobiotics and jeopardize health.

Besides Cyp, the flavin-containing monooxygenase (Fmo) is another major group of Phase I drug-metabolizing enzymes catalyzing the oxidative biotransformation of drugs. Fmo enzymes break down compounds that contain nitrogen, sulfur, or phosphorus. Fmo3, a major Fmo isoform, plays an important role in metabolizing drugs such as the anticancer drug tamoxifen, the pain medication codeine, the antifungal drug ketoconazole, and antipsychotic drugs clozapine and olanapine (Ciraulo et al., 2005; Klick and Hines, 2007; Parte and Kupfer, 2005). In our study, GBE inhibited the expression of Fmo3 remarkably with the high dose treatment (77-fold reduction detected by microarray and 166-fold reduction validated by TaqMan assay). These results suggest that down-regulated expression of the Fmo3 enzyme by GBE potentially inhibits metabolism of certain drugs resulting in drug-drug or drug-food interactions, thus reducing the therapeutic effects or enhancing the toxicity induced by their metabolites.

It is worth noting that while the microarray studies on the changes of drug metabolizing enzyme expression in kava-treated rats (Guo et al., 2009) and kava-treated mice (Guo et al., submitted for publication) used a 90-day treatment of kava, the present GBE study was performed over a two-year period of treatment. The difference in time of herbal treatment suggests that the effect of such a dietary supplement on drug metabolizing enzymes is a persistent phenomenon (up to two years). Our previous study with kava and the present study with *Ginkgo biloba* provide substantial evidence that the two herbal dietary supplements cause remarkable changes in drug metabolizing enzymes, particularly the Cyp isozymes, raising the possibility that these herbal supplements might profoundly affect the pharmacokinetics of many co-administrated drugs or other food supplements, thus leading to hepatotoxicity.

In addition to the investigation of alteration for many drug metabolizing genes, in this study we also explored pathways and networks in response to GBE treatment and found that *Ginkgo biloba* exposure resulted in the significant stimulation of the Nrf2-mediated oxidative pathway (Figure 6) and the alteration of the Myc regulated pathway (Figure 7).

A previous study found that long-term exposure to kava could result in the perturbation of the Nrf2-mediated pathway and eventually generate reactive oxygen species (ROS). In this study, *Ginkgo biloba* treatments also stimulated the Nrf2-mediated oxidative stress response pathway ($P = 0.005$). Keap1-Nrf2-ARE signaling plays a critical role in protecting cells from endogenous and exogenous stresses, and is involved in antioxidative response, detoxification of xenobiotics, and proteome maintenance (Kensler et al., 2007). Under normal physiological conditions the transcription factor Nrf2 localizes in the cytoplasm and interacts with Keap1. Upon oxidative stress, Nrf2 is released from Keap1 and translocates to the nucleus and subsequently activates its various downstream target genes (Kensler et al., 2007). The target genes show a wide spectrum of functions, such as inactivating oxidants, increasing the levels of glutathione, and enhancing toxin export via transporters to enhance cell survival. As illustrated in Figure 6, in response to GBE treatment, Nrf2 regulated genes including various Gst genes which are involved in GSH-conjugate formation were altered. The Gst genes (Gsta2, Gsta4, Gstms, and Gstp1) and Ugt1a2 were all up-regulated following GBE treatment. In turn, the resulting enhancement of GST enzymes is used for neutralizing the electrophiles, the process considered generally as an important detoxification mechanism. NADPH-dependent enzyme NQO1 was also up-regulated, which has protective roles toward detoxification of xenobiotic carbonyls and quinones. GBE treatment also elevated Gsr (glutathione reductase) gene expression, and GSR regulates cellular GSH homeostasis by catalyzing the reduction of GSSG to GSH using NADPH as a reducing cofactor (Harvey et al., 2009) In addition, GBE treatment reduced the activity of Sod3, which is one of the superoxide dismutases (SODs) that are the most important line of antioxidant enzyme defense systems against ROS and particularly superoxide anion radicals (Zelko et al., 2002). Studies using Nrf2 knock-out mice showed that they are more susceptible to acetaminophen-induced hepatocellular injury (Chan et al., 2001) and benzo[a]pyrene-induced tumor formation with higher levels of DNA adducts (Ramos-Gomez et al., 2001). This susceptibility is partly due to a reduced level in the expression of detoxification enzymes (Aleksunes and Manautou, 2007; Kensler et al., 2007). Activation of detoxification enzymes plays a pivotal role in protecting cells from oxidative insult when cells encounter a toxin challenge.

Based on the network analysis, 34 genes were incorporated into the first network in response to GBE treatment (Figure 7). The key molecule in this most significantly changed network was Myc pro-oncogene with 5.7-fold increased expression. The protein encoded by this gene is a multifunctional, nuclear phosphoprotein that plays a role in cell cycle progression, apoptosis and cellular transformation. It functions as a transcription factor that regulates

transcription of specific target genes. It has been established that stimulation of Myc pathways can cause liver damage, leading to severe lesions up to the tumorigenic level. Overexpression of Myc has been frequently observed in tumors and is the early and critical event in the pathogenesis of hepatocellular carcinoma (Beer et al., 2008;Dang, 1999;Pelengaris et al., 2002). A study using a transgenic model indicated that overexpression of the c-Myc gene sufficiently induced hepatic proliferation and tumorigenesis (Beer et al., 2008;Sandgren et al., 1989). Many studies have shown that Myc gene overexpression during hepatocarcinogenesis induced by carcinogens including choline-devoid diet, arsenite, 5-diethoxycarbonyl-1,4-dihydrocollidine (DDC) and carbon tetrachloride (CCl4) (Beer et al., 2008;Chandar et al., 1989;Chen et al., 2001). In addition, DDC and carbon tetrachloride cooperate with Myc to promote hepatocyte proliferation and rapidly uncover the onset of liver cancer (Beer et al., 2008). Using a toxicogenomic approach to study the molecular mechanisms of non-genotoxic carcinogenicity revealed that major pathways linked to cancer were interconnected via Myc (Nie et al., 2006), and the high percentage of gene expression signature linked to Myc suggested the important role of the Myc gene. Therefore, the alteration of Myc-mediated pathways may serve as potential predictors in carcinogenicity. Among 34 genes incorporated into the Myc-centered network (Figure 7), over 60% of the genes (21 genes) were reported to be directly associated with Myc and most of these genes function in cell cycle, cell growth/proliferation, and cell death processes. The Myc associated gene, Gas1 (growth arrest-specific 1) was found to be 20-fold down-regulated. Gas1, the tumor suppressor gene which plays role in growth suppression by blocking entry to S phase, is directly inhibited at the transcriptional level by Myc (Lee et al., 1997), and the transcriptional repression of growth arrest genes is one step in the promotion of cell growth. Down-regulation was also one of the distinct events in the process of EGF (Epidermal Growth Factor) induced hepatocarcinogenesis (Borlak et al., 2005). The loss of growth control through Gas1 may be a necessary event in the multi-step neoplastic transformation.

In summary, we analyzed gene expression profiles in the liver of mice treated with *Ginkgo biloba*, a widely sold product in health food stores in the United States. Using the systematic approaches of HCA, PCA, pathway analysis, and network analysis, we identified 129, 289, and 2,011 genes that were differentially expressed in the livers of 300, 600, and 2,000 mg/kg GBE-treated mice, respectively, and observed that a significant portion of the changed genes were associated with metabolism, Nrf2-mediated oxidative stress, and the Myc gene centered network. Based on our results, we speculate that long term exposure of *Ginkgo biloba* may cause hepatic damage, including severe liver lesions and even liver tumors, further studies are warranted.

Acknowledgments

We thank Drs. Tucker A. Patterson and James C. Fuscoe for their critical review of this manuscript. This article is not an official guidance or policy statement of the National Toxicology Program (NTP) or U.S. Food and Drug Administration (FDA). No official support or endorsement by the FDA and NTP is intended or should be inferred. This research was supported in part by the Intramural Research Program of the NIH, National Institute of Environmental Health Sciences.

References

ALEKSUNES LM, MANAUTOU JE. Emerging role of Nrf2 in protecting against hepatic and gastrointestinal disease. Toxicol Pathol 2007;35:459–473. [PubMed: 17562481]

BEER S, KOMATSUBARA K, BELLOVIN DI, KUROBE M, SYLVESTER K, FELSHER DW. Hepatotoxin-induced changes in the adult murine liver promote MYC-induced tumorigenesis. PLoS ONE 2008;3:e2493. [PubMed: 18560566]

BLOMME EA, YANG Y, WARING JF. Use of toxicogenomics to understand mechanisms of drug-induced hepatotoxicity during drug discovery and development. Toxicol Lett 2009;186:22–31. [PubMed: 18996174]

BORLAK J, MEIER T, HALTER R, SPANEL R, SPANEL-BOROWSKI K. Epidermal growth factor-induced hepatocellular carcinoma: gene expression profiles in precursor lesions, early stage and solitary tumours. Oncogene 2005;24:1809–1819. [PubMed: 15674348]

BRESSLER R. Herb-drug interactions: interactions between kava and prescription medications. Geriatrics 2005;60:24–25. [PubMed: 16153141]

BRUNNBERG S, ANDERSSON P, LINDSTAM M, PAULSON I, POELLINGER L, HANBERG A. The constitutively active Ah receptor (CA-Ahr) mouse as a potential model for dioxin exposure--effects in vital organs. Toxicology 2006;224:191–201. [PubMed: 16766111]

CHAN K, HAN XD, KAN YW. An important function of Nrf2 in combating oxidative stress: detoxification of acetaminophen. Proc Natl Acad Sci USA 2001;98:4611–4616. [PubMed: 11287661]

CHAN PC, FU PP. Toxicity of Panax ginseng-An herbal medicine and dietary supplements. J Food Drug Anal 2007;15:416–427.

CHAN PC, XIA Q, FU PP. Ginkgo biloba leave extract: biological, medicinal, and toxicological effects. J Environ Sci Health C Environ Carcinog Ecotoxicol Rev 2007;25:211–244. [PubMed: 17763047]

CHANDAR N, LOMBARDI B, LOCKER J. c-Myc gene amplification during hepatocarcinogenesis by a choline-devoid diet. Proc Natl Acad Sci USA 1989;86:2703–2707. [PubMed: 2649891]

CHEN H, LIU J, ZHAO CQ, DIWAN BA, MERRICK BA, WAALKES MP. Association of c-myc overexpression and hyperproliferation with arsenite-induced malignant transformation. Toxicol Appl Pharmacol 2001;175:260–268. [PubMed: 11559025]

CIRAULO, DA.; SHADER, RI.; GREENBLATT, DJ.; CREELMAN, W. Drug interaction in Psychiatry. Lippincott Williams & Wilkins; 2005.

CLAYTON NP, YOSHIZAWA K, KISSLING GE, BURKA LT, CHAN PC, NYSKA A. Immunohistochemical analysis of expressions of hepatic cytochrome P450 in F344 rats following oral treatment with kava extract. Exp Toxicol Pathol 2007;58:223–236. [PubMed: 17059882]

CLOUATRE DL. Kava kava: examining new reports of toxicity. Toxicol Lett 2004;150:85–96. [PubMed: 15068826]

DANG CV. c-Myc target genes involved in cell growth, apoptosis, and metabolism. Mol Cell Biol 1999;19:1–11. [PubMed: 9858526]

DUBEY AK, SHANKAR PR, UPADHYAYA D, DESHPANDE VY. Ginkgo biloba--an appraisal. Kathmandu Univ Med J 2004;2:225–229.

FDA. FDA advises dietary supplement manufacturers to remove comfrey products from the market. 2001 [July 6, 2001]. Available at: http://www.cfsan.fda.gov/~dms/supplmnt.html

FDA. FDA Public Health News, FDA announced major initiatives for dietary supplements. 2004a

FDA. Final rule declaring dietary supplements containing ephedrine alkaloids adulterated because they present an unreasonable risk federal register. 2004

FONG HH. Integration of herbal medicine into modern medical practices: issues and prospects. Integr Cancer Ther 2002;1:287–293. [PubMed: 14667286]

FU PP. Quality assurance and safety of herbal dietary supplements. J Food Drug Anal 2007;15:333–334.

FU PP, XIA Q, CHOU MW, LIN G. Detection, hepatotoxicity, and tumorigenicity of pyrrolizidine alkaloids in Chinese herbal plants and herbal dietary supplemnets. J Food Drug Anal 2007;15:400–415.

FU PP, XIA Q, GUO L, YU H, CHAN PC. Toxicity of kava kava. J Environ Sci Health Part C 2008;26:89–112.

FU PP, YANG YC, XIA Q, CHOU MW, CUI YY, LIN G. Pyrrolizidine alkaloids - tumorigenic components in Chinese herbal medicines and dietary supplements. J Food Drug Anal 2002;10:198–211.

GONZALEZ FJ, GELBOIN HV. Role of human cytochromes P450 in the metabolic activation of chemical carcinogens and toxins. Drug Metab Rev 1994;26:165–183. [PubMed: 8082563]

GONZALEZ FJ, YU AM. Cytochrome P450 and xenobiotic receptor humanized mice. Annu Rev Pharmacol Toxicol 2006;46:41–64. [PubMed: 16402898]

GUO L, LI Q, XIA Q, DIAL S, CHAN PC, FU P. Analysis of gene expression changes of drug metabolizing enzymes in the livers of F344 rats following oral treatment with kava extract. Food Chem Toxicol 2009;47:433–442. [PubMed: 19100306]

GUO L, LOBENHOFER EK, WANG C, SHIPPY R, HARRIS SC, ZHANG L, et al. Rat toxicogenomic study reveals analytical consistency across microarray platforms. Nat Biotechnol 2006;24:1162–1169. [PubMed: 17061323]

GURLEY BJ, GARDNER SF, HUBBARD MA, WILLIAMS DK, GENTRY WB, CARRIER J, et al. In vivo assessment of botanical supplementation on human cytochrome P450 phenotypes: Citrus aurantium, Echinacea purpurea, milk thistle, and saw palmetto. Clin Pharmacol Ther 2004;76:428–440. [PubMed: 15536458]

GURLEY BJ, GARDNER SF, HUBBARD MA, WILLIAMS DK, GENTRY WB, CUI Y, et al. Clinical assessment of effects of botanical supplementation on cytochrome P450 phenotypes in the elderly: St John's wort, garlic oil, Panax ginseng and Ginkgo biloba. Drugs Aging 2005;22:525–539. [PubMed: 15974642]

GURLEY BJ, SWAIN A, BARONE GW, WILLIAMS DK, BREEN P, YATES CR, et al. Effect of goldenseal (Hydrastis canadensis) and kava kava (Piper methysticum) supplementation on digoxin pharmacokinetics in humans. Drug Metab Dispos 2007;35:240–245. [PubMed: 17079360]

HARVEY CJ, THIMMULAPPA RK, SINGH A, BLAKE DJ, LING G, WAKABAYASHI N, et al. Nrf2-regulated glutathione recycling independent of biosynthesis is critical for cell survival during oxidative stress. Free Radic Biol Med 2009;46:443–453. [PubMed: 19028565]

HU Z, YANG X, HO PC, CHAN SY, HENG PW, CHAN E, et al. Herb-drug interactions: a literature review. Drugs 2005;65:1239–1282. [PubMed: 15916450]

IYER KR, SINZ MW. Characterization of Phase I and Phase II hepatic drug metabolism activities in a panel of human liver preparations. Chem Biol Interact 1999;118:151–169. [PubMed: 10359459]

KENSLER TW, WAKABAYASHI N, BISWAL S. Cell survival responses to environmental stresses via the Keap1-Nrf2-ARE pathway. Annu Rev Pharmacol Toxicol 2007;47:89–116. [PubMed: 16968214]

KLICK DE, HINES RN. Mechanisms regulating human FMO3 transcription. Drug Metab Rev 2007;39:419–442. [PubMed: 17786630]

LEE TC, LI L, PHILIPSON L, D ZIFF EB. Myc represses transcription of the growth arrest gene gas1. Proc Natl Acad Sci USA 1997;94:12886–12891. [PubMed: 9371770]

LIVAK KJ, SCHMITTGEN TD. Analysis of relative gene expression data using real-time quantitative PCR and the 2(-Delta Delta C(T)) Method. Methods 2001;25:402–408. [PubMed: 11846609]

MARTIGNONI M, GROOTHUIS GM, DE KANTER R. Species differences between mouse, rat, dog, monkey and human CYP-mediated drug metabolism, inhibition and induction. Expert Opin Drug Metab Toxicol 2006;2:875–894. [PubMed: 17125407]

MATTHIAS A, BLANCHFIELD JT, PENMAN KG, BONE KM, TOTH I, LEHMANN RP. Permeability studies of Kavalactones using a Caco-2 cell monolayer model. J Clin Pharm Ther 2007;32:233–239. [PubMed: 17489874]

NIE AY, MCMILLIAN M, PARKER JB, LEONE A, BRYANT S, YIEH L, et al. Predictive toxicogenomics approaches reveal underlying molecular mechanisms of nongenotoxic carcinogenicity. Mol Carcinog 2006;45:914–933. [PubMed: 16921489]

NTP. Nomination of Ginkgo biloba extract. 1998. Available at: http://ntp.niehs.nih.gov/?objectid=BDCABE80-123F-7908-7BF75015B4AC13D

PARTE P, KUPFER D. Oxidation of tamoxifen by human flavin-containing monooxygenase (FMO) 1 and FMO3 to tamoxifen-N-oxide and its novel reduction back to tamoxifen by human cytochromes P450 and hemoglobin. Drug Metab Dispos 2005;33:1446–1452. [PubMed: 15987777]

PELENGARIS S, KHAN M, EVAN G. c-MYC: more than just a matter of life and death. Nat Rev Cancer 2002;2:764–776. [PubMed: 12360279]

RAMOS-GOMEZ M, KWAK MK, DOLAN PM, ITOH K, YAMAMOTO M, TALALAY P, et al. Sensitivity to carcinogenesis is increased and chemoprotective efficacy of enzyme inducers is lost in nrf2 transcription factor-deficient mice. Proc Natl Acad Sci USA 2001;98:3410–3415. [PubMed: 11248092]

REZEN T, CONTRERAS JA, ROZMAN D. Functional genomics approaches to studies of the cytochrome p450 superfamily. Drug Metab Rev 2007;39:389–399. [PubMed: 17786628]

ROYMANS D, VAN LOOVEREN C, LEONE A, PARKER JB, MCMILLIAN M, JOHNSON MD, et al. Determination of cytochrome P450 1A2 and cytochrome P450 3A4 induction in cryopreserved human hepatocytes. Biochem Pharmacol 2004;67:427–437. [PubMed: 15037195]

SANDGREN EP, QUAIFE CJ, PINKERT CA, PALMITER RD, BRINSTER RL. Oncogene-induced liver neoplasia in transgenic mice. Oncogene 1989;4:715–724. [PubMed: 2543942]

SHI L, REID LH, JONES WD, SHIPPY R, WARRINGTON JA, BAKER SC, et al. The MicroArray Quality Control (MAQC) project shows inter- and intraplatform reproducibility of gene expression measurements. Nat Biotechnol 2006;24:1151–1161. [PubMed: 16964229]

SINGH YN. Potential for interaction of kava and St. John's wort with drugs. J Ethnopharmacol 2005;100:108–113. [PubMed: 16005588]

TUSHER VG, TIBSHIRANI R, CHU G. Significance analysis of microarrays applied to the ionizing radiation response. Proc Natl Acad Sci U S A 2001;98:5116–21. [PubMed: 11309499]

WANG A, GEHAN EA. Gene selection for microarray data analysis using principal component analysis. Stat Med 2005;24:2069–2087. [PubMed: 15806617]

WILLIAMSON EM. Interactions between herbal and conventional medicines. Expert Opin Drug Saf 2005;4:355–378. [PubMed: 15794726]

WOLD RS, LOPEZ ST, YAU CL, BUTLER LM, PAREO-TUBBEH SL, WATERS DL, et al. Increasing trends in elderly persons' use of nonvitamin, nonmineral dietary supplements and concurrent use of medications. J Am Diet Assoc 2005;105:54–63. [PubMed: 15635346]

XU C, LI CY, KONG AN. Induction of phase I, II and III drug metabolism/transport by xenobiotics. Arch Pharm Res 2005;28:249–268. [PubMed: 15832810]

ZELKO IN, MARIANI TJ, FOLZ RJ. Superoxide dismutase multigene family: a comparison of the CuZn-SOD (SOD1), Mn-SOD (SOD2), and EC-SOD (SOD3) gene structures, evolution, and expression. Free Radic Biol Med 2002;33:337–349. [PubMed: 12126755]

ZOU L, HARKEY MR, HENDERSON GL. Effects of herbal components on cDNA-expressed cytochrome P450 enzyme catalytic activity. Life Sci 2002;71:1579–1589. [PubMed: 12127912]

ZURER P, HANSON D. Chemistry puts herbal supplements to the test. Chemical & Engineering News 2004;82:16.

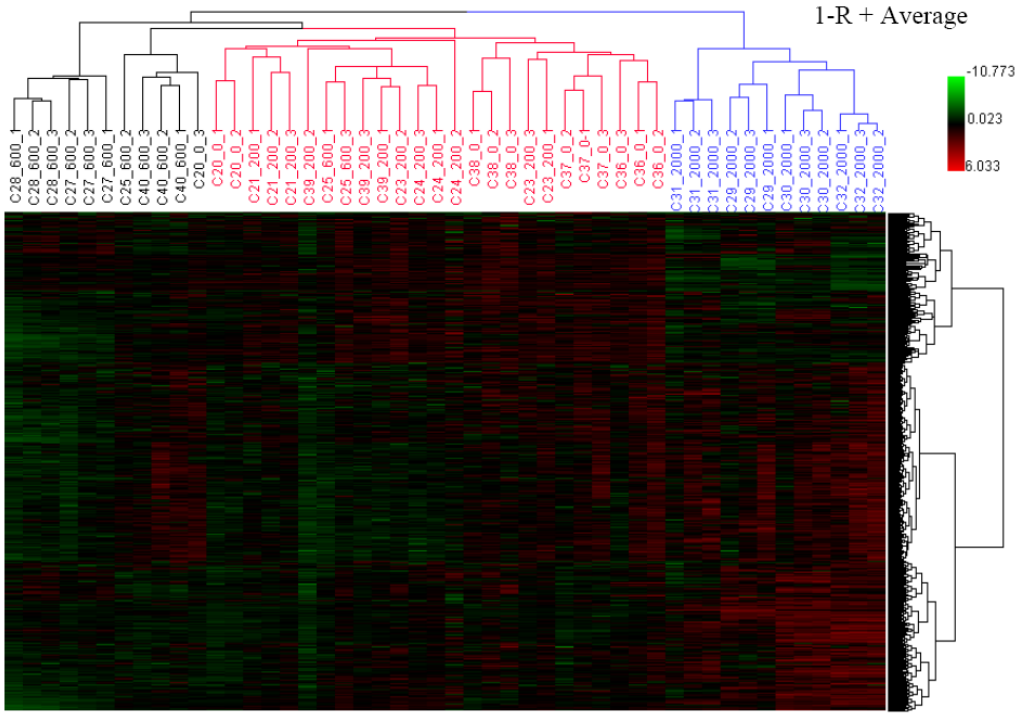

Figure 1.

Hierarchical Cluster Analysis (HCA) of expression profiles for control and GBE-treated groups. Each column represents the results from an individual hybridization. Each row represents the $\log_2$ intensity values of the 48 samples for one particular gene. Samples are labeled according to the convention of Animal ID_Dose (mg/kg)_Technical replicate number.

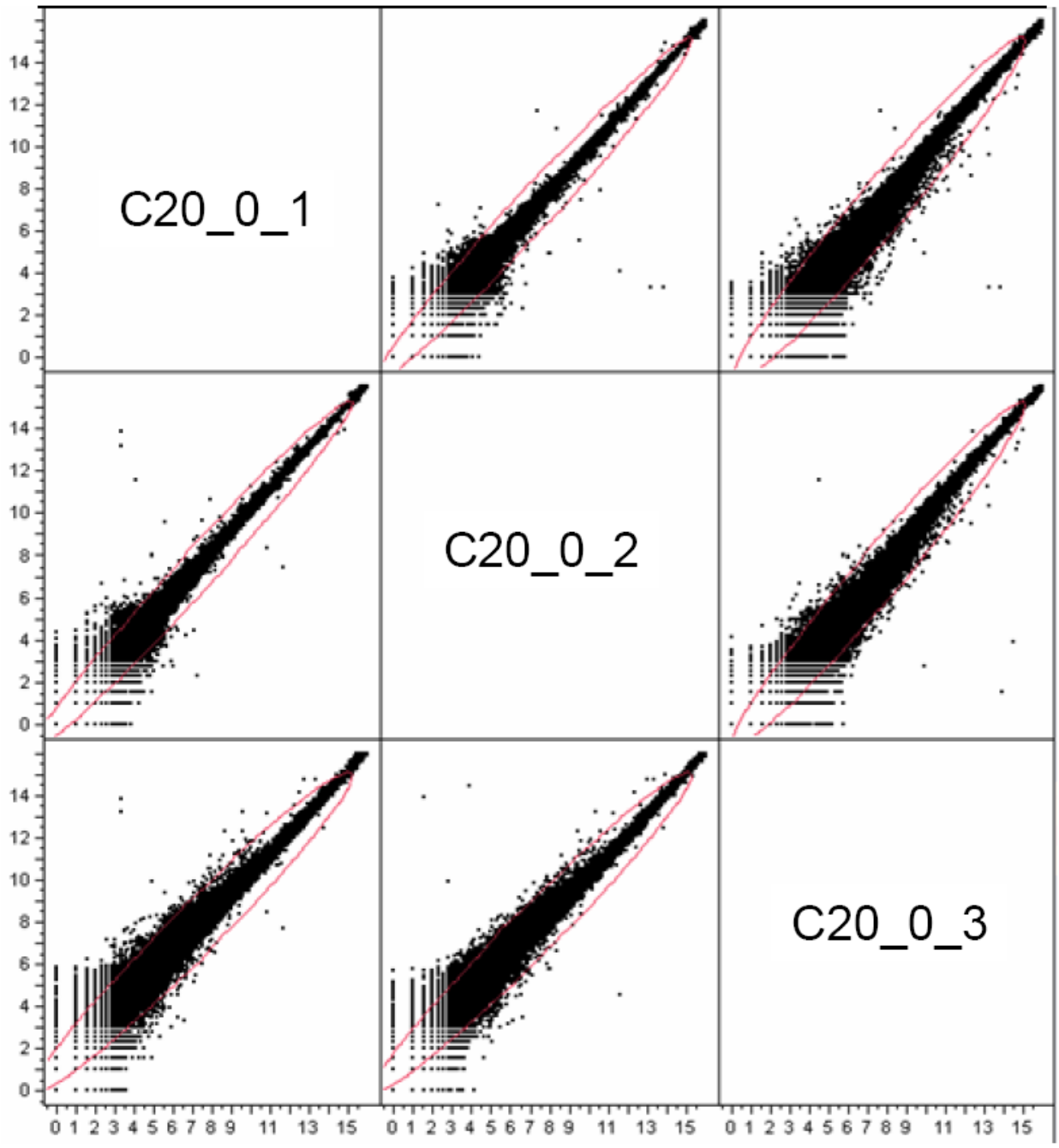

Figure 2.
The $\log_2$ raw intensity data of the three technical replicates (C20_0_1, C20_0_2, and C20_0_3) were plotted against each other.

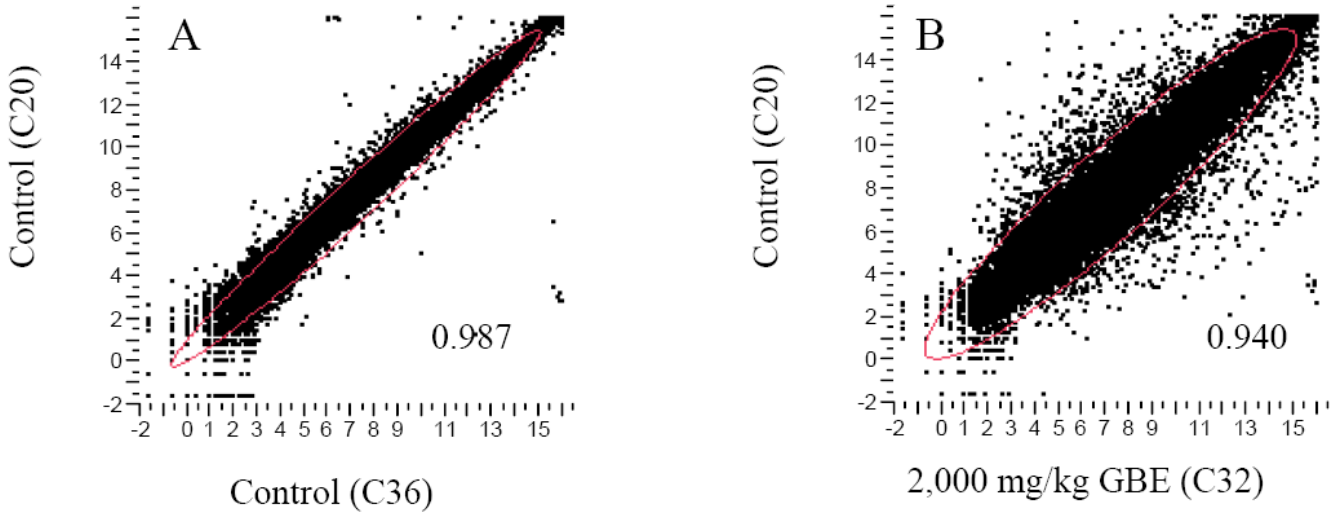

Figure 3.
Overall gene expression profiles. The $\log_2$ transformed intensity was used for scatter plotting. A: two control samples (C20 and C36); B: control (C20) and 2,000 mg/kg GBE (C32) treated sample were plotted against each other.

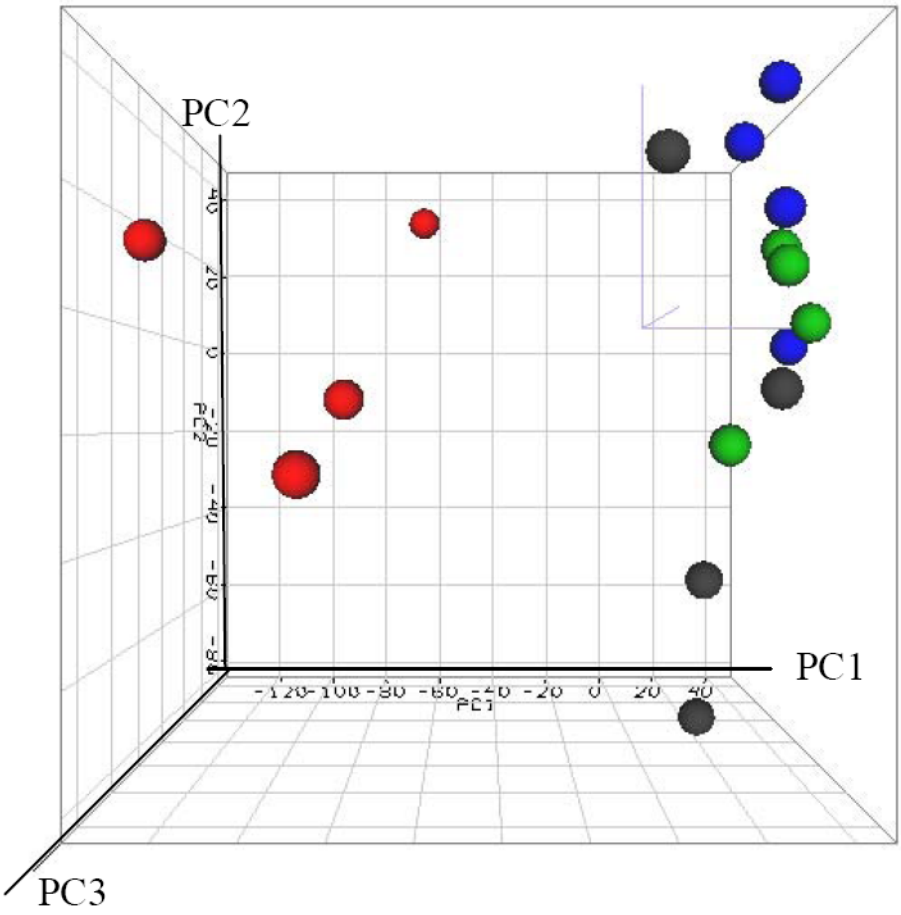

Figure 4.
Principal Component Analysis (PCA) of gene expression profiles for GBE - treated groups and the concurrent controls. The intensity of the entire gene set was used; no specific cutoff was applied for the analysis. The autoscaled method was used for the PCA. The blue, green, black and red dots indicate control, 200, 600 and 2000 mg/kg treatment, respectively. PC1, PC2, and PC3 represent first principal component, second principal component, and third principal component.

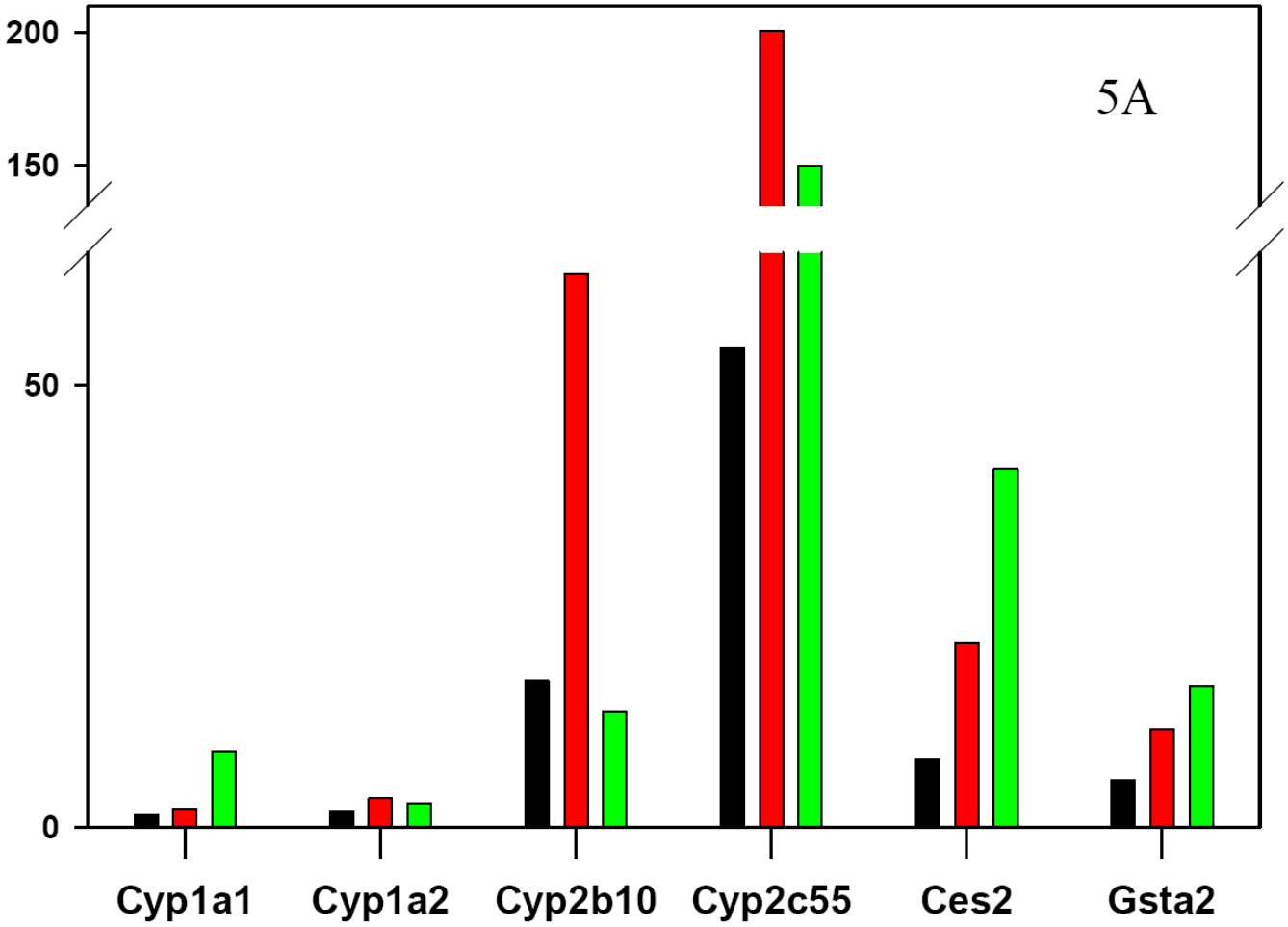

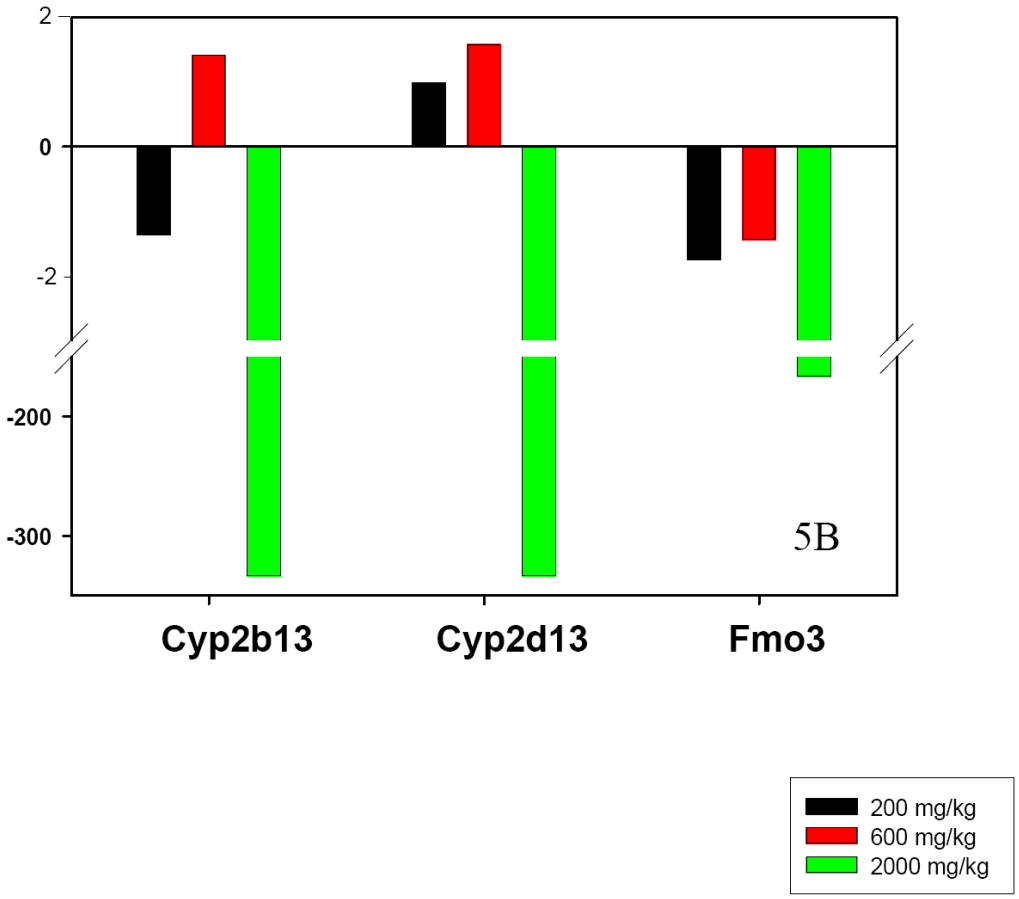

Figure 5.
TaqMan assays of the gene expression changes; (A) Cyp1a1, Cyp1a2, Cyp2b10, Cyp2c55, Ces2, and Gsta2; and (B) Cyp2d13; Cyp2b13, and Fmo3.

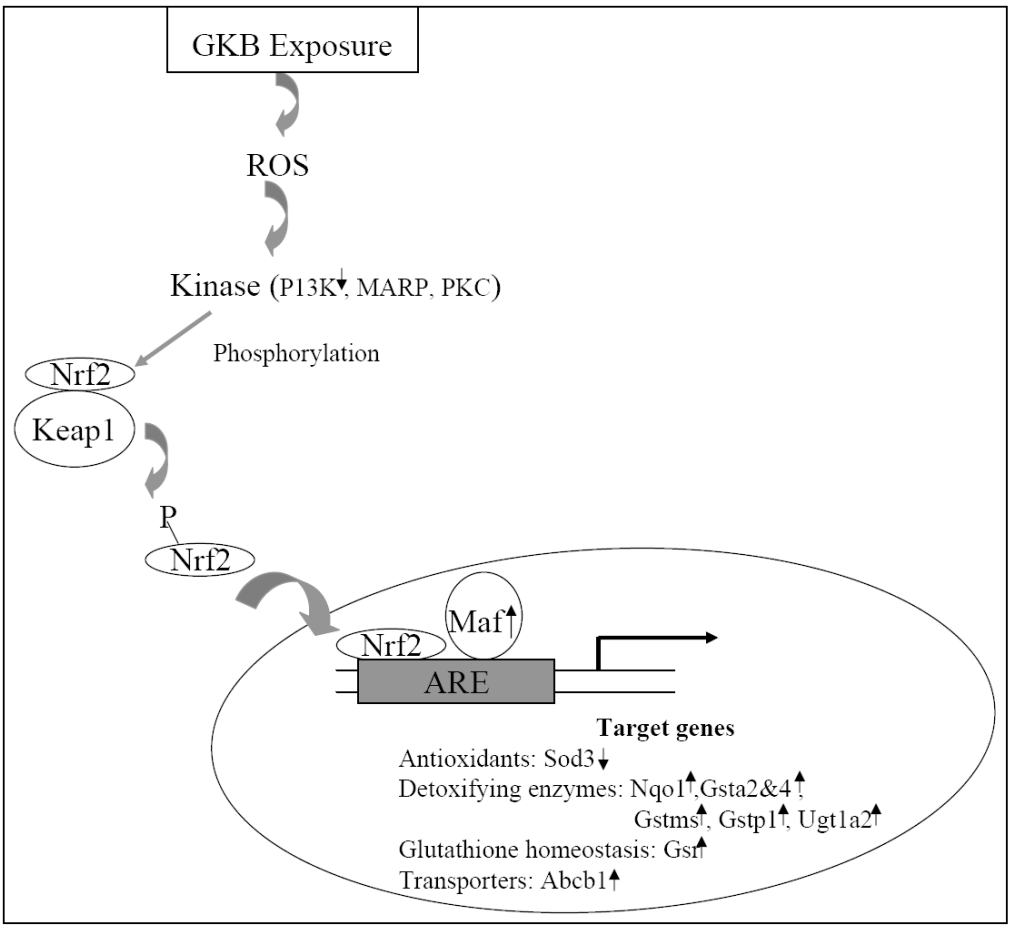

Figure 6.
Alteration of NRF2 (nuclear factor erythroid-related factor 2)-mediated oxidative stress response.

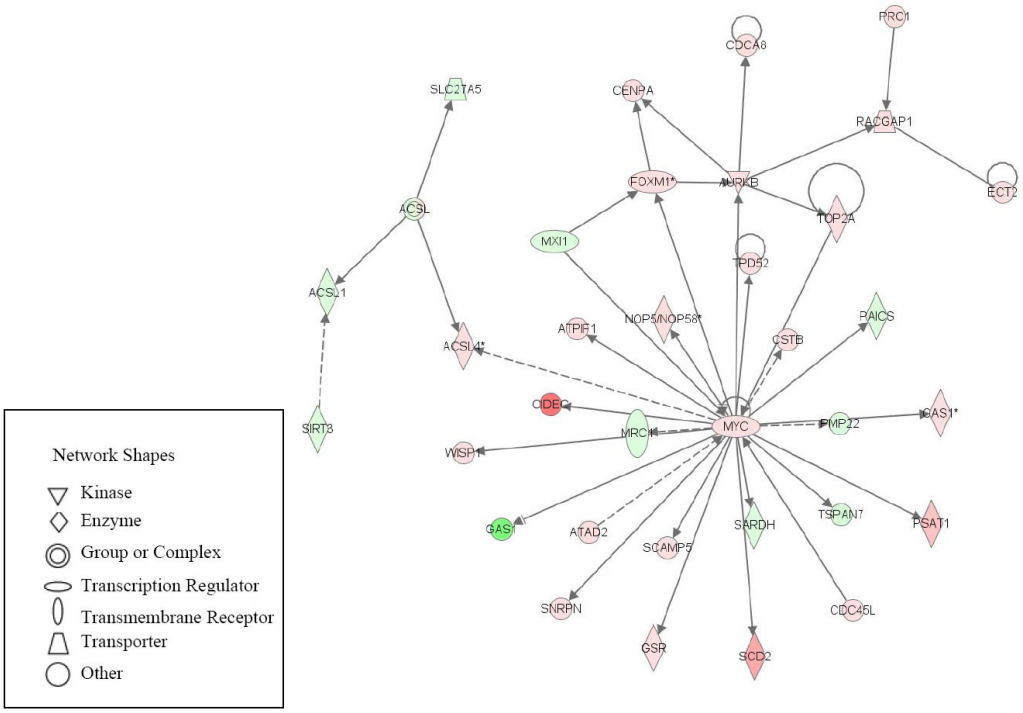

Figure 7.

The first network (cell cycle, cellular movement and cancer) containing 34 differentially expressed genes. Green indicates down-regulation and red indicates up-regulation. Solid lines indicate direct interactions and dashed lines indicate indirect interactions between tw

Table 1

Assessment of microarray data quality (technical replicates): The microarray data reproducibility was assessed by the Pearson correlation coefficient of pair-wise $\log_2$ intensity correlation among 3 technical replicates (1, 2, and 3). The R value of 3 technical replicates is shown. Pearson correlation matrix of arrays was calculated based on all data points (31,802 probes).

Sample#	Dose (mg/kg)	R values, Median
C20_1,2,3	0	0.992, 0.991, 0.998
C36_1,2,3	0	0.995, 0.991, 0.996
C37_1,2,3	0	0.992, 0.990, 0.997
C38_1,2,3	0	0.979, 0.979, 0.997
C21_1,2,3	200	0.991, 0.987, 0.996
C23_1,2,3	200	0.992, 0.984, 0.994
C24_1,2,3	200	0.965, 0.961, 0.997
C39_1,2,3	200	0.997, 0.996, 0.998
C25_1,2,3	600	0.990, 0.990, 0.997
C27_1,2,3	600	0.992, 0.992, 0.997
C28_1,2,3	600	0.995, 0.993, 0.997
C40_1,2,3	600	0.993, 0.990, 0.994
C29_1,2,3	2000	0.984, 0.982, 0.990
C30_1,2,3	2000	0.988, 0.988, 0.997
C31_1,2,3	2000	0.990, 0.990, 0.994
C32_1,2,3	2000	0.995, 0.995, 0.997

Table 2

Assessment of microarray data quality (biological replicates). The microarray data reproducibility was assessed by the Pearson correlation coefficient of pair-wise $\log_2$ intensity correlation. Pearson correlation matrix of 16 arrays was calculated based on all data points (31,802 probes).

	C20-0	C36-0	C37-0	C38-0	C21-200	C23-200	C24-200	C39-200	C25-600	C27-600	C28-600	C40-600	C29-2000	C30-2000	C31-2000	C32-2000
C20-0	1.000	0.988	0.988	0.986	0.987	0.987	0.979	0.976	0.976	0.983	0.973	0.985	0.958	0.959	0.960	0.939
C36-0		1.000	0.988	0.985	0.988	0.987	0.978	0.977	0.973	0.978	0.971	0.985	0.957	0.963	0.964	0.944
C37-0			1.000	0.983	0.985	0.986	0.976	0.976	0.973	0.974	0.965	0.985	0.956	0.958	0.960	0.940
C38-0				1.000	0.984	0.986	0.979	0.978	0.974	0.985	0.979	0.978	0.952	0.957	0.958	0.933
C21-200					1.000	0.989	0.983	0.981	0.980	0.981	0.975	0.984	0.959	0.962	0.959	0.940
C23-200						1.000	0.984	0.987	0.980	0.981	0.973	0.982	0.956	0.963	0.964	0.939
C24-200							1.000	0.980	0.977	0.978	0.972	0.973	0.961	0.966	0.957	0.940
C39-200								1.000	0.986	0.973	0.967	0.969	0.945	0.954	0.952	0.926
C25-600									1.000	0.975	0.969	0.972	0.951	0.953	0.949	0.930
C27-600										1.000	0.988	0.977	0.960	0.963	0.958	0.941
C28-600											1.000	0.969	0.955	0.957	0.951	0.933
C40-600												1.000	0.968	0.967	0.963	0.955
C29-2000													1.000	0.977	0.961	0.970
C30-2000														1.000	0.970	0.973
C31-2000															1.000	0.962
C32-2000																1.000

Table 3

Genes involved in 3 Phases of liver drug metabolism altered by 2,000 mg/kg GBE treatment.

Gene Symbol	Locus Link ID	Gene Description	Fold Change	P Value
		Phase I		
Adh7	11529	alcohol dehydrogenase 7 (class IV), mu or sigma polypeptide	2.5	0.006
Aldh5a1	214579	aldhehyde dehydrogenase family 5, subfamily A1	-2.9	0.002
Aldh8a1	237320	aldehyde dehydrogenase 8 family, member A1	-2.8	0.005
Cyp1a1	13076	cytochrome P450, family 1, subfamily a, polypeptide 1	6.8	0.001
Cyp1a2	13077	cytochrome P450, family 1, subfamily a, polypeptide 2	2.3	0.008
Cyp2a12	13085	cytochrome P450, family 2, subfamily a, polypeptide 12	-2.2	0.004
Cyp2a5	13087	cytochrome P450, family 2, subfamily a, polypeptide 5	2.9	0.005
Cyp2b10	13088	cytochrome P450, family 2, subfamily b, polypeptide 10	17.3	0.001
Cyp2b13	13089	cytochrome P450, family 2, subfamily b, polypeptide 13	-38.5	0.004
Cyp2b20	13088	cytochrome P450, family 2, subfamily b, polypeptide 10	14.6	0
Cyp2b9	13094	cytochrome P450, family 2, subfamily b, polypeptide 9	-18.9	0.009
Cyp2c29	13095	cytochrome P450, family 2, subfamily c, polypeptide 29	3.6	0
Cyp2c55	72082	cytochrome P450, family 2, subfamily c, polypeptide 55	50.2	0
Cyp2c66	69888	cytochrome P450, family 2, subfamily c, polypeptide 66	4.4	0.001
Cyp2d13	68444	cytochrome P450, family 2, subfamily d, polypeptide 13	-29.4	0.003
Cyp2f2	13107	cytochrome P450, family 2, subfamily f, polypeptide 2	-13.2	0
Cyp2g1	13108	cytochrome P450, family 2, subfamily g, polypeptide 1	-2.1	0.009
Cyp2j5	13109	cytochrome P450, family 2, subfamily j, polypeptide 5	-7.1	0
Cyp2j9	74519	cytochrome P450, family 2, subfamily j, polypeptide 9	-14.9	0
Cyp2u1	71519	cytochrome P450, family 2, subfamily u, polypeptide 1	-17.9	0.008
Cyp3a16	13114	cytochrome P450, family 3, subfamily a, polypeptide 16	-8.4	0.003
Cyp3a41	53973	cytochrome P450, family 3, subfamily a, polypeptide 41	-2.3	0.009
Cyp46a1	13116	cytochrome P450, family 46, subfamily a, polypeptide 1	-8.9	0.001
Cyp4f14	64385	cytochrome P450, family 4, subfamily f, polypeptide 14	-4.8	0.006
Cyp4f16	70101	cytochrome P450, family 4, subfamily f, polypeptide 16	2.9	0.001
Cyp51	13121	cytochrome P450, family 51	2.0	0.002
Dhrs3	20148	dehydrogenase/reductase (SDR family) member 3	-2.0	0.003

OMICS. Author manuscript; available in PMC 2010 July 30.

Gene Symbol	Locus Link ID	Gene Description	Fold Change	P Value
Dhrs9	241452	dehydrogenase/reductase (SDR family) member 9	3.6	0.001
Dpyd	99586	dihydropyrimidine dehydrogenase	-3.8	0
Fmo3	14262	flavin containing monooxygenase 3	-76.9	0.001
Maoa	17161	monoamine oxidase A	6.3	0.008
Maob	109731	monoamine oxidase B	-2.4	0.001
Ptgs1	19224	prostaglandin-endoperoxide synthase 1	-2.5	0.004
		Phase II		
Acsl1	14081	acyl-CoA synthetase long-chain family member 1	-3.1	0.005
Acsl4	50790	acyl-CoA synthetase long-chain family member 4	5.2	0
Ces2	234671	carboxylesterase 2	24.7	0
Ephx1	13849	epoxide hydrolase 1, microsomal	2.5	0.002
Gsta2	14858	glutathione S-transferase, alpha 2 (Yc2)	34.6	0.001
Gsta4	14860	glutathione S-transferase, alpha 4	2.6	0.006
Gstk1	76263	glutathione S-transferase kappa 1	-2.2	0.004
Gstm1	14862	glutathione S-transferase, mu 1	2.8	0.002
Gstm2	14863	glutathione S-transferase, mu 2	4.4	0.004
Gstm3	14864	glutathione S-transferase, mu 3	11.5	0
Gstm4	14865	glutathione S-transferase, mu 4	4.4	0.007
Gstm6	14867	glutathione S-transferase, mu 6	5.2	0.002
Gsto1	14873	glutathione S-transferase omega 1	-4.7	0.003
Gstp1	14870	glutathione S-transferase, pi 1	4.4	0
Nnmt	18113	nicotinamide N-methyltransferase	-10.4	0
Nqo3a2	72017	cytochrome b5 reductase 1	3.2	0
Sult1d1	53315	sulfotransferase family 1D, member 1	-2.7	0.006
Sult3a1	57430	sulfotransferase family 3A, member 1	-35.7	0
		Phase III		
Abcb1a	18671	ATP-binding cassette, sub-family B (MDR/TAP), member 1A	2.3	0.004
Abcc12	244562	ATP-binding cassette, sub-family C (CFTR/MRP), member 12	5.5	0.009
Abcc2	12780	ATP-binding cassette, sub-family C (CFTR/MRP), member 2	3.1	0.004
Abcc4	239273	ATP-binding cassette, sub-family C (CFTR/MRP), member 4	18.9	0.001

Gene Symbol	Locus Link ID	Gene Description	Fold Change	P Value
Abcc5	27416	ATP-binding cassette, sub-family C (CFTR/MRP), member 5	7.5	0.001
Abcc6	27421	ATP-binding cassette, sub-family C (CFTR/MRP), member 6	-3.0	0.006
Abcd3	19299	ATP-binding cassette, sub-family D (ALD), member 3	-2.3	0.006
Aqp6	11831	aquaporin 6	2.2	0.003
Aqp7	11832	aquaporin 7	17.8	0.001
Mvp	78388	major vault protein	2.7	0
Slc10a1	20493	solute carrier family 10 (sodium/bile acid cotransporter family), member 1	-4.4	0.002
Slc22a3	20519	solute carrier family 22 (organic cation transporter), member 3	10.2	0.004
Slc22a7	108114	solute carrier family 22 (organic anion transporter), member 7	-4.4	0.005
Slc29a1	63959	solute carrier family 29 (nucleoside transporters), member 1	-2.4	0.005
Slc2a1	20525	solute carrier family 2 (facilitated glucose transporter), member 1	2.0	0.002
Slc3a1	20532	solute carrier family 3, member 1	-4.2	0.009
Slc7a5	20539	solute carrier family 7 (cationic amino acid transporter, y+ system), member 5	3.3	0.002

Table 4

Numbers of changed Phase I, Phase II, and Phase III genes after 2,000 mg/kg GBE treatment.

	Genes presented on array	Genes altered by GBE treatment (%)
Phase I	154	33 (21%)
Phase II	87	18 (21%)
Phase III	72	17 (24%)
Total drug metabolizing genes	313	68 (22%)

OMICS. Author manuscript; available in PMC 2010 July 30.

Table 5

Top 20 Canonical pathways altered by GBE treatment

	Canonical Pathway	*P*-value
1	Metabolism of Xenobiotics by Cytochrome P450	1.26E-11
2	Fatty Acid Metabolism	4.57E-09
3	Tryptophan Metabolism	1.74E-07
4	LPS/IL-1 Mediated Inhibition of RXR Function	2.04E-07
5	Arachidonic Acid Metabolism	2.57E-07
6	Linoleic Acid Metabolism	3.09E-06
7	Aryl Hydrocarbon Receptor Signaling	9.77E-06
8	Xenobiotic Metabolism Signaling	1.91E-04
9	Glutathione Metabolism	4.57E-04
10	Aminosugars Metabolism	1.38E-03
11	PXR/RXR Activation	1.74E-03
12	NRF2-mediated Oxidative Stress Response	5.37E-03
13	Hepatic Fibrosis / Hepatic Stellate Cell Activation	1.07E-02
14	Tyrosine Metabolism	1.35E-02
15	Acute Phase Response Signaling	2.29E-02
16	FXR/RXR Activation	2.40E-02
17	Sphingolipid Metabolism	3.47E-02
18	G-Protein Coupled Receptor Signaling	4.68E-02
19	Coagulation System	4.79E-02
20	Glycosaminoglycan Degradation	5.89E-02